*Physiol Genomics* 52: 121–132, 2020.
First published December 23, 2019; doi:10.1152/physiolgenomics.00087.2019.

**RESEARCH ARTICLE** | *The Microbiome-Human Host Interactions Contributing to Cardiovascular and Inflammatory Disease*

# Transcriptomic signature of gut microbiome-contacting cells in colon of spontaneously hypertensive rats

**Tao Yang,[1] Hongbao Li,[1,3] Aline C. Oliveira,[1] Ruby Goel,[1] Elaine M. Richards,[1] Carl J. Pepine,[2] and Mohan K. Raizada[1]**

[1]*Department of Physiology and Functional Genomics, Department of Medicine, College of Medicine, University of Florida, Gainesville, Florida;* [2]*Division of Cardiovascular Medicine, Department of Medicine, College of Medicine, University of Florida, Gainesville, Florida; and* [3]*Department of Physiology and Pathophysiology, School of Basic Medical Sciences, Xi'an Jiaotong University, Xi'an, China*

Submitted 27 August 2019; accepted in final form 20 December 2019

**Yang T, Li H, Oliveira AC, Goel R, Richards EM, Pepine CJ, Raizada MK.** Transcriptomic signature of gut microbiome-contacting cells in colon of spontaneously hypertensive rats. *Physiol Genomics* 52: 121–132, 2020. First published December 23, 2019; doi:10.1152/physiolgenomics.00087.2019.—Fecal matter transfer from hypertensive patients and animals into normotensive animals increases blood pressure, strengthening the evidence for gut-microbiota interactions in the control of blood pressure. However, cellular and molecular events involved in gut dysbiosis-associated hypertension remain poorly understood. Therefore, our objective in this study was to use gene expression profiling to characterize the gut epithelium layer in the colon in hypertension. We observed significant suppression of components of T cell receptor (TCR) signaling in the colonic epithelium of spontaneously hypertensive rats (SHR) when compared with Wistar Kyoto (WKY) normotensive rats. Western blot analysis confirmed lower expression of key proteins including T cell surface glycoprotein CD3 gamma chain (Cd3g) and lymphocyte cytosolic protein 2 (Lcp2). Furthermore, lower expression of cytokines and receptors responsible for lymphocyte proliferation, differentiation, and activation (e.g., *Il12r*, *Il15ra*, *Il7*, *Il16*, *Tgfb1*) was observed in the colonic epithelium of the SHR. Finally, *Alpi* and its product, intestinal alkaline phosphatase, primarily localized in the epithelial cells, were profoundly lower in the SHR. These observations demonstrate that the colonic epithelium undergoes functional changes linked to altered immune, barrier function, and dysbiosis in hypertension.

colonic epithelium; gene expression profile; hypertension; TCR signaling pathway

## INTRODUCTION

Since a link between gut dysbiosis and hypertension was first demonstrated (57), the primary investigational focus of the field has been to validate this concept using a variety of animal models of hypertension and patients with high blood pressure (56, 62). Collectively, these studies have led to the conclusion that the investigation of the mechanisms involved in impaired host-microbiota communication could be the key to understanding the involvement of gut dysbiosis in hypertension. The colon harbors significantly more bacteria compared with other gastrointestinal segments. Proximal colon is close to the cecum, the site with high bacterial fermentation. Our previous publications demonstrate that not only the fecal microbiota but also the metabolic capacity of the microbiota differs between hypertensive and normotensive subjects (50, 57). Therefore, the current study focuses on host proximal colonic epithelium, the layer intimately and constantly interacting with gut microbiota and its metabolites that may mediate the previously reported physiological changes (8, 26, 48, 49, 54).

Gut epithelium, a critical mediator of intestinal homeostasis, forms a physiological and immunological barrier, segregating commensal gut microbiota and their products from the host (39, 55). The epithelium is chronically exposed to environmental hypertension risk factors (e.g., diet, salt, toxins, drugs), gut microbiota, and their metabolites. Thus, it is an ideal target for genetically and epigenetically mediated influences on host-microbiota cross talk. Furthermore, intraepithelial lymphocytes (IELs), intrinsic cells of the gut epithelial layer, form the first line of host immune defense in the gut (6). This is particularly relevant since 70–80% of body's immune cells reside in the gut (59), and significant involvement of immune processes in hypertension has been evident (35, 48). IELs are activated yet resting T cells (16), characterized by expression of activation markers (6) and gut-homing integrins (14), which immediately release cytokines upon encountering antigen. IELs are increased in autoimmune enteropathies and inflammatory bowel diseases, etc. (30). Thus, gut epithelium has both a dynamic epithelial barrier function and an IEL immune defense system (40, 44).

Mutual host-microbiota cross talk has been the subject of extensive investigation primarily focused on elucidating the mechanisms by which effectors and modulators originating in the gut microbiota influence the intestinal epithelium (1, 56). Furthermore, altered functions of the intestinal epithelium have been demonstrated to change the composition of the gut microbiota (53). However, in hypertension, little is known about this bidirectional cross-communication between gut epithelium and microbiota, despite established dysbiosis and gut pathology in hypertension. Therefore, we used normotensive Wistar Kyoto (WKY) rat and spontaneously hypertensive rat (SHR),

Address for reprint requests and other correspondence: M. K. Raizada, Dept. of Physiology and Functional Genomics, Univ. of Florida College of Medicine, PO Box 100274, Gainesville, FL 32610 (e-mail: mraizada@ufl.edu).

since the SHR was one of the first animal hypertension models demonstrated to exhibit gut dysbiosis. Our objectives of the present study included *1*) evaluate the changes in the gut in prehypertensive SHR, *2*) perform RNA-Seq of colonic epithelium to compare and contrast gene expression profiles between WKY and SHR, and *3*) identify and characterize pathways associated with immune cells and epithelial cells that are altered in the SHR. We present evidence of altered T cell receptor (TCR) signaling, profoundly less intestinal alkaline phosphatase (IAP) and their implications in hypertension.

## MATERIALS AND METHODS

*Animals.* The study conforms to the University of Florida Institutional Animal Care and Use Committee guidelines and the National Institutes of Health Guide for the Care and Use of Laboratory Animals. Eight-week-old male WKY and SHR/NCrl were purchased as breeding parents from Charles River Laboratories (Wilmington, MA) and housed in a temperature-controlled room (22–23°C) on a 12:12 h light-dark cycle at the McKnight Brain Institute of the University of Florida. Two rats per cage were kept in specific pathogen-free, positive-ventilated cages with access to irradiated food (#7912; Envigo, Indianapolis, IN) and sterile water ad libitum. Rats were housed with autoclaved corn-cob bedding (Laboratory Supply, Fort Worth, TX). The resulting offspring were used in this study. SHR and its normotensive control WKY are well-established rat model for hypertension studies. Blood pressure was measure by tail cuff with the BP-2000 blood pressure analysis system (Visitech System, Apex, NC).

*Colonic epithelium isolation.* Colonic epithelia were isolated as previously described (15). Briefly, freshly obtained proximal colon was sequentially incubated with *1*) Hanks' balanced salt solution (HBSS) (VWR, Radnor, PA) containing 1.5 mM dithiothreitol and 3 mM ethylenediaminetetraacetic acid (EDTA) on ice for 20 min and *2*) HBSS containing 1.5 mM EDTA at 37°C for 10 min. Then the tissue was shaken for 3 min to separate the epithelium from the tissue. Epithelium suspension was centrifuged at 1,500 rpm at 4°C and washed with HBSS containing 10% fetal bovine serum. The cells obtained were aliquoted and stored at −80°C until RNA was extracted.

To generate single-cell suspensions for flow cytometry, we incubated isolated cells with prewarmed dispase (5 U/mL) buffer (Fisher Scientific, Hampton, NH) containing 50 μg/mL of DNase I (Thermo Fisher, Waltham, MA) at 37°C for 10 min. After incubation, cells were washed with FACS buffer and filtered through 100 μm cell strainers.

*RNA-Seq library preparation and sequencing.* The cells derived from proximal colonic epithelium layer of each of four rats per group (8 preparations in total) were lysed, and total RNA was extracted with an RNeasy plus mini kit (QIAGEN, Germantown, MD) according to the manufacturer's protocol. RNA concentration was determined on Qubit 2.0 Fluorometer (ThermoFisher), and RNA quality was assessed with the Agilent 2100 Bioanalyzer (Agilent Technologies, Santa Clara, CA). Total RNA with 28S/18S $>$ 1 and RNA integrity numbers between 7.1 and 9.3 were used for RNA-Seq library construction.

RNA-Seq libraries were constructed with the NEBNext Ultra Directional RNA Library Prep Kit for Illumina (New England Biolabs, Ipswich, MA) following the manufacturer's instructions. Briefly, 500 ng of total RNA was used for mRNA isolation using NEBNext Poly(A) mRNA Magnetic Isolation module (New England Biolabs). Purified mRNA was used to construct RNA library with the NEBNext Ultra II Directional Library Prep kit (New England Biolabs). Briefly, RNA was fragmented in NEBNext First Strand Synthesis Buffer by heating at 94°C. This step was followed by first-strand cDNA synthesis using reverse transcriptase and oligo(dT) primers. Subsequently, synthesis of double-stranded cDNA was performed, followed by end-repair and adaptor ligation. At this point, Illumina adaptors were ligated to the sample. Finally, the library with a unique barcode was enriched by 10 cycles of amplification and purified by Agencourt AMPure beads (Beckman Coulter, Brea, CA). The library was sized on the bioanalyzer and quantitated by Qubit.

In preparation for sequencing on the HiSeq3000 Illumina sequencer, the eight uniquely barcoded libraries were normalized to 2.5 nM and equimolar amounts pooled. The RNA-Seq library pool was spiked with 1% of the PhiX library. Library pools were processed according to the Illumina HiSeq3000 protocol for clustering on the cBOT machine. After denaturation, neutralization, and mixing with the ExAmp reagent, the final pool concentration for clustering was 0.25 nM. Sequencing was done using a 2 × 101 cycles format (paired-end configuration). A typical sequencing run in the HiSeq3000 produced 600 million to 650 paired-end reads per lane.

The obtained sequencing data have been deposited to NCBI Gene Expression Omnibus with reference number GSE 130671 (https://www.ncbi.nlm.nih.gov/geo/query/acc.cgi?acc=GSE130671).

*RNA-Seq bioinformatics analysis.* The quality of the RNA-Seq sequence data was first evaluated using FastQC (11) before further downstream analysis. Low-quality sequences were removed, and reads with lower quality were trimmed with Trimmomatic (2). Star Aligner (7) was used to map high-quality paired-end reads to the latest rat genome, Rnor_6.0. Gene expression was obtained with RSEM. The expected read counts and Fragments Per Kilobase of transcript per Million mapped reads (FPKM) were extracted for further analysis. The estimated read counts were taken as input for edgeR to perform differential expression analysis using generalized linear models. The thresholds for calling significantly differentially expressed genes were set at false discovery rate (FDR) $<$ 0.05, fold change 2, and the average FPKM of at least one for each comparison group higher than 0.

Among the genes with FDR $<$ 0.05, only genes with FDR $<$ 0.01 were included in the subsequent functional network and gene ontology analyses.

Functional network analysis was performed using Cytoscape (version 3.6.1) with STRING and CentiScape 2.2 plugins. Gene ontology analysis was performed with WebGestalt (WEB-based GEne SeT AnaLysis Toolkit) as described previously (51, 60).

*Western blot and antibodies.* Primary antibodies for Western blots were purchased from Santa Cruz Biotechnology (Dallas, TX): CD3G (sc-393271), SLP-76 (F7, sc-13157), LAT (11B.12, sc-53550), and Abcam (Cambridge, UK): GAPDH (6C5, ab8245). Secondary antibodies were purchased from LI-COR Biosciences (Lincoln, NE): IRDye 680RD (goat anti-rabbit, 926-6807) and IRDye 800CW (Goat anti-mouse, 926-32210).

Cell pellet was lysed in RIPA buffer in the presence of proteinase inhibitors (P8340, MilliporeSigma, Burlington, MA). After debris was spun out, supernatant was collected and protein concentration was measured by the Bradford method (#5000006; Bio-Rad, Hercules, CA). We loaded 20 mg of protein, after denaturation, into each well for protein electrophoresis at a constant voltage of 120 V until bromophenol blue reached the bottom of the gel. Proteins were transferred to PVDF membrane (#1620264, Bio-Rad) using a Trans-Blot Semi-Dry Electrophoretic Transfer Cell (#1703940, Bio-Rad) with a constant voltage of 25 V for 15 min. Membranes were briefly washed with PBS and then incubated with primary antibodies at 4°C overnight at 1:1,000 dilution. After being washed three times for 10 min with PBS containing 0.05% Tween 20, membranes were incubated with secondary antibodies at room temperature for 1 h before being scanned on LI-COR Odyssey.

*Identification of differentially expressed genes and biological functions.* For RNA-Seq gene expression data, the FDR was set at 0.05. All genes with FDR $<$0.05 are presented in the supplemental Excel file.

For functional network and ontology analyses, differentially expressed genes between SHR and WKY with FDR $< 0.01$ were used, and the results are shown in Fig. 1.

For biological processes enriched in colonic epithelium of WKY, only the top 10 processes (FDR $< 0.0001$) are presented in Table 1, due to the considerable numbers of processes enriched in WKY. In SHR, only three biological processes were enriched with a lower stringency FDR of 0.1, presented in Table 1.

*Single cell preparation from spleen and mesenteric lymph nodes.* Mesenteric lymph nodes (MLN) and spleen were dissected, homogenized, and then separated with 100 μm strainers. Pelleted cells were suspended in the red blood cell lysis buffer and rotated at room temperature for 10 min to eliminate red cells. After being washed with FACS buffer, pelleted cells were stained.

*Flow cytometry and antibodies.* Isolated epithelial cells were stained with antiepithelial cell adhesion marker (EpCAM) antibody (ab187276; Abcam, Cambridge, UK) at 4°C overnight, followed by secondary antibody AF488 goat anti-rabbit (A11034; ThermoFisher, Waltham, MA) incubation at room temperature for 45min.

Cells from epithelium, MLN, and spleen ($n = 4$/group) were stained with antibodies: Live/Dead fixable violet dead cell stain kit (L34963, ThermoFisher), AF647 anti-rat TCR αβ (20116, Biolegend, San Diego, CA), FITC anti-rat CD8a (201703, Biolegend), and PE anti-rat TCR γδ (202605, Biolegend). A total number of 30,000 cells

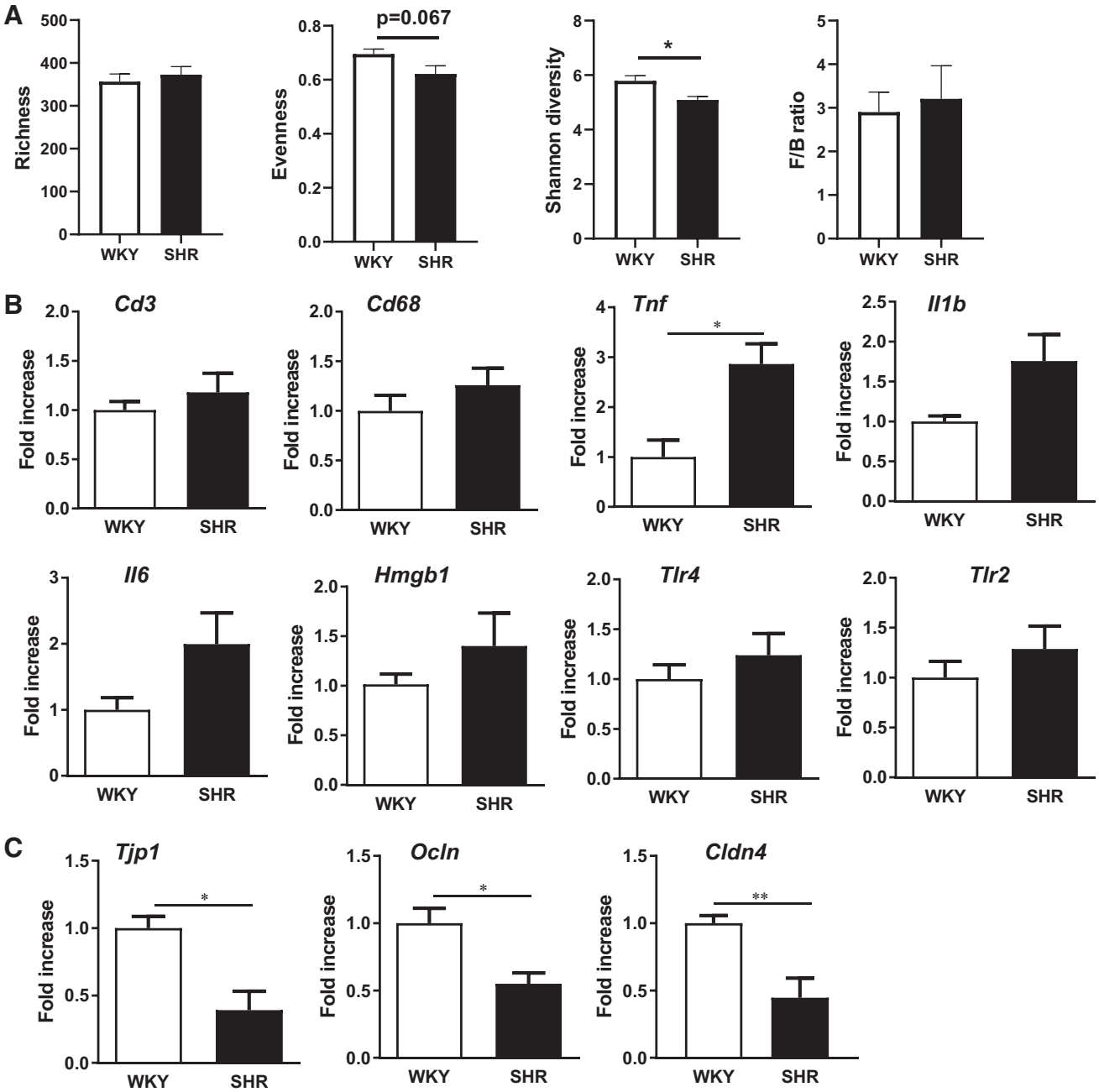


Fig. 1. Colonic changes in prehypertensive spontaneously hypertensive rats (SHR). *A*: comparison of gut microbial diversity and Firmicutes-Bacteroidetes (F/B) ratio between 3 wk old SHR and age-matched Wistar Kyoto (WKY). *B*: evaluation of inflammation-related markers in the proximal colon of 3 wk old SHR and age-matched WKY. *C*: evaluation of tight junction protein expression in the proximal colon of 3 wk old SHR and age-matched WKY. Statistical analysis was performed by unpaired *t* test $*P < 0.05$. $n = 6$/group.

Table 1. *Differential biological processes between WKY and SHR epithelium*

| Biological Process | ID | Genes in Gene Set /Total Genes in Category | Adjusted *P* Value (FDR) |
|---|---|---|---|
| | *Enriched in WKY* | | |
| Single organism cell adhesion | GO0098602 | 40/469 | 1.88e-10 |
| Leukocyte activation | GO0045321 | 38/429 | 1.88e-10 |
| Homeostasis of number of cells | GO0048872 | 18/144 | 9.94e-07 |
| Immune effector process | GO0002252 | 28/348 | 1.14e-06 |
| Regulation of cell activation | GO0050865 | 24/284 | 4.48e-06 |
| Positive regulation of immune system process | GO0002684 | 32/482 | 6.25e-06 |
| Hematopoietic or lymphoid organ development | GO0048534 | 31/481 | 1.7e-05 |
| Regulation of immune response | GO0050776 | 26/364 | 2.17e-05 |
| Leukocyte proliferation | GO0070661 | 16/162 | 6.39e-05 |
| Negative regulation of immune system process | GO0002683 | 19/228 | 7.62e-05 |
| | *Enriched in SHR* | | |
| Response to lipid | GO0033993 | 18/902 | 7.46e-02 |
| Response to lipopolysaccharide | GO0032496 | 10/298 | 7.46e-02 |
| Response to molecule of bacterial origin | GO0002237 | 18/902 | 7.46e-02 |

Genes with significant differences between Wistar Kyoto (WKY) and spontaneously hypertensive rats (SHR) were used to predict the biological functions enriched in WKY and SHR, respectively. Top 10 and top 3 enriched biological processes are presented.

per sample were analyzed on BD LSR II cytometer (BD, Franklin Lakes, NJ).

*IAP immunostaining and quantification.* Colon samples were collected and fixed in 10% formaldehyde in PBS for 24 h. We stained 5 μm sections with Anti-Alkaline phosphatase primary antibody (1:200, Boster). For IAP detection, VECTASTAIN Elite ABC kit PK-7200 (Vector Laboratories, Burlingame, CA) was used according to the manufacturer's protocol. Briefly, sections were washed with PBS with 0.3% Triton X-100, followed by incubation in peroxidase block solution (BLOXALL, Vector Laboratories) for 10 min. After being blocked for 1 h in normal horse serum, samples were incubated overnight at 4°C with primary antibody. The next day, sections were washed, incubated for 1 h at room temperature in biotinylated horse anti-rabbit/mouse secondary antibody, followed by R.T.U VECTASTAIN Elite ABC Reagent, rinsed, and then exposed to 3-3′diaminobenzidine (DAB) as the chromogenic peroxidase substrate. As control of immunohistochemistry detection, we evaluated the absence of primary antibody or omission of secondary antibody incubation and no immunostaining was detected under these conditions. Finally, the sections were washed in PBS, dehydrated, and coverslipped with Cytoseal (Stephens Scientific, Wayne, NJ). Sections were examined under bright-field illumination with an Olympus photomicroscope with a ×40 objective. The intensity of DAB immunoreactivity in the epithelial cells was analyzed in 15–20 crypts/rat with image analysis software Fiji (ImageJ). Images were normalized by using an algorithm, converting the intensity of the optical density (OD) with the following formula: OD = log(max intensity/mean intensity), where max intensity = 255 for 8-bit images.

Supplemental data are available at https://doi.org/10.6084/m9.figshare.9731573.

## RESULTS

*Colonic changes in prehypertensive SHR.* First, we determined changes in the colon of 3 wk old SHR since their systolic blood pressure (SBP) was comparable to age-matched WKY (Supplemental Fig. S1A). Analysis of microbiota showed no significant differences in Firmicutes-Bacteroidetes ratio or richness when compared with age-matched WKY Fig. 1*A*), a finding consistent with previous observations (43). However, diversity was significantly lower in 3 wk old SHR (Fig. 1*A*). Although there was no change in the proinflammatory markers *Cd3* (a marker for T lymphocytes), *Cd68* (a marker for macrophages), Il1b, Il6, *Hmgb1* (an inflammatory effector downstream of TLR2 and TLR4), *Tlr4* (a receptor for Gram-negative bacterial lipopolysaccharide, LPS), or *Tlr2* (a receptor for Gram-positive bacterial lipoteichoic acid), there was ~2-fold more *Tnf* in the prehypertensive SHR (Fig. 1*B*). Interestingly, there were fewer tight junction proteins (i.e., *Tjp1*, *Ocln*, *Cldn4*) (Fig. 1*C*), confirming previous data (43). Therefore, these colonic changes in prehypertensive SHR suggest that disruption of the gut barrier occurs before the development of hypertension.

*Distinct global gene expression patterns in the colonic epithelium of WKY and SHR.* Next, we performed RNA-Seq to determine complete gene expression profiles in the 16 wk old SHR with established hypertension and compare them with their normotensive WKY counterparts. The SBP of SHR was 189 ± 5 mmHg compared with 121 ± 4 mmHg of WKY (Supplemental Fig. S1C). RNA from epithelia of four animals per group were sequenced with 39,289,562.3 ± 1,526,679.6 raw reads per rat and an average of 86.7 ± 0.5% uniquely mapped reads per rat. RNA-Seq of colonic epithelium revealed significant differences between the normotensive WKY rat and the hypertensive SHR. Overall, we observed lower expression of differentially expressed genes (blue nodes) in the SHR (Fig. 2*A*). In gene interaction analyses, these genes fell into four major groups (dashed circles). In addition, the top eight genes with the most interactions with other genes within the four major groups were identified as hub genes within the network, numbered 1–8 in Fig. 2*A*. These were *Lck* (lymphocyte-specific protein tyrosine kinase), *Gng4* (G protein subunit gamma 4), *CD3g* (T cell surface glycoprotein CD3 gamma chain), *Zap70* (zeta chain of T cell receptor-associated protein kinase 70), *Il2rb* (interleukin-2 receptor subunit beta), *Cxcr4* (C-X-C motif chemokine receptor 4), *Tgfb1* (transforming growth factor beta 1), and *Ifit1* (interferon-induced protein with tetratricopeptide repeats 1) (Fig. 2*A*), all of which are involved in immune responses. Similar to the overall change, the major networks were predominantly downregulated in the SHR, as the expression levels of most genes within the networks were reduced (Fig. 2*A*). There are also genes with limited interac-

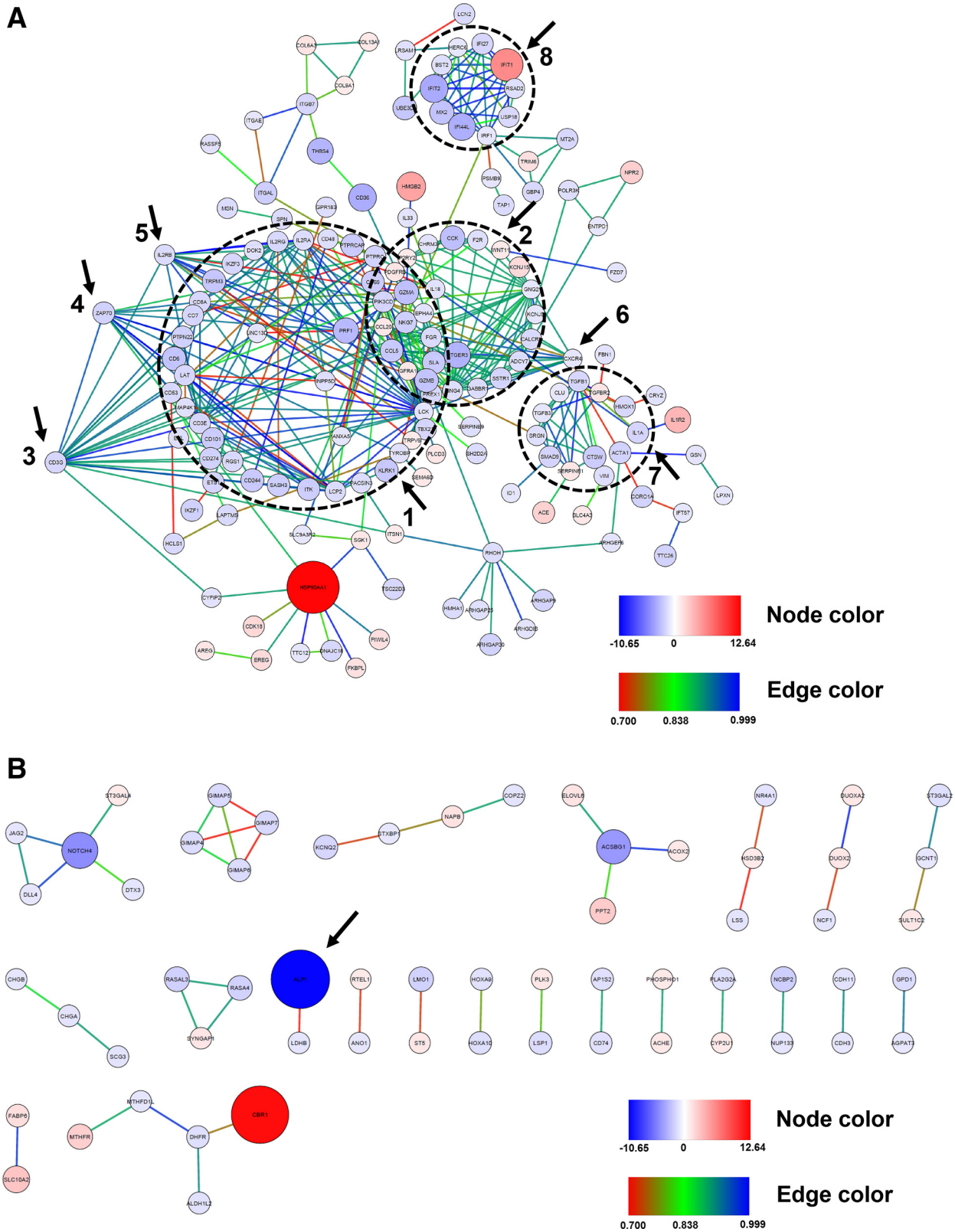


Fig. 2. Altered, primarily suppressed, gene expression in the colonic epithelium of SHR. *A*: major subnetworks and hub genes, identified by their complex interaction with multiple genes, are indicated by dashed circles and numbered arrows, respectively. Node size represents the fold change of SHR over WKY, while the color blue indicates reduced expression, and red indicates higher expression in the SHR. The edge color expresses how tight the interaction was between the linked nodes, with red indicating loose interaction, blue indicating close interaction. *B*: minor subnetworks of genes with a significant difference between WKY and SHR. Genes interacting with a limited number of other genes were shown. Node size represents the fold change of SHR over WKY, while the color blue indicates reduced expression, and red indicates higher expression in the SHR. The edge color expresses how tight the interaction was between the linked nodes, with red indicating loose interaction, blue indicating close interaction.

tions, including *Alpi*, that were expressed more abundantly in WKY, indicated by the arrow (Fig. 2*B*).

We next analyzed overall functional changes of altered gene expression profiles: genes with significantly higher (fold change $> 2$; FDR $< 0.01$) expression in the WKY epithelium were subjected to biological process analysis with WEB-based Gene SeT AnaLysis Toolkit (WebGestalt) (51, 60). We annotated 247 out of 412 genes and used them for the functional enrichment analysis. The top 10 biological processes enriched in the WKY colonic epithelium are presented in Table 1. Cell adhesion, leukocyte activation, homeostasis of number of cells, immune effector process, hematopoietic or lymphoid organ development, and leukocyte proliferation indicate the enrichment of functions relevant to leukocyte proliferation and activation in the WKY (Table 1). In addition, regulation of cell activation, positive regulation of immune system process, regulation of immune response, and negative regulation of immune system process indicate that mechanisms regulating immune responses were more in the WKY compared with the SHR (Table 1).

In contrast, only when an FDR of $<0.1$ was accepted there were enriched biological processes modeled from the SHR data, and then only three. They include response to LPS, response to lipid, and response to molecule of bacterial origin (Table 1).

*Abnormal TCR signaling pathway in the colonic epithelium of SHR.* To study functional changes associated with seven hub genes in the WKY and SHR epithelium, the seven hub genes and their network-associated genes were subjected to functional enrichment analysis in the open resource STRING (46). The expression level of *Lck* and its interacting genes were generally lower in the SHR (Supplemental Fig. S2A). In addition, *Lck* closely interacted with other genes indicated by edge colors from green to blue (Supplemental Fig. S2A). The major KEGG (Kyoto Encyclopedia of Genes and Genomes) pathways related to this network were TCR signaling, natural killer cell-mediated cytotoxicity, and primary immunodeficiency (Table 2). *Gng4* closely interacted with its associated genes whose expression was mainly lower in the SHR (Supplemental Fig. S2B). The KEGG pathways linked to these genes were chemokine signaling pathway, neuroactive ligand-receptor interaction, and morphine addiction (Table 2). *CD3g* and *Zap70*, another two hub genes, were also lower in the SHR (Supplemental Fig. S2, C and D). Remarkably, these two genes were both closely associated with TCR signaling, natural killer cell-mediated cytotoxicity, and primary immunodeficiency, the same functional pathways as the *Lck* network (Table 2). Moreover, *Il2rb* and closely associated *Il2ra* and *Il2rg* were all downregulated in the SHR (Supplemental Fig. S2E). IL2 signaling has been indicated in proliferation, differentiation, and cell growth of T lymphocytes. We observed a significant lower expression in the transcripts of three IL2 core receptor subunits in SHR epithelium. Considering the suppressed expression of hub signaling genes (i.e., *Lck*, *Zap70*) of the TCR pathway, the lower expression of IL2 receptor subunits further suggested alterations in the T cell population in the SHR (Table 2).

Major genes mediating the cellular TCR signaling pathway are summarized based on the FPKM mapped reads in RNA-Seq data. Significant reductions in transcripts for *CD3e*, *CD3g*, *Lck*, *Zap70*, *Lcp2*, and *Lat* were found in the SHR colonic epithelium (Fig. 3*A*). Canonical TCR αβ signaling is composed of a phosphorylation cascade of cellular factors, including LCK, ZAP70, LAT, and LCP2 in activated T cells. To confirm the changes in TCR signaling, Western blotting was performed to determine the levels of *CD3g*, *Lcp2*, and *Lat* proteins in SHR colonic epithelium. Consistent with the transcriptional changes, we observed a significantly lower expression of CD3G and LCP2 in the colonic epithelium of SHR (Fig. 3*B*). Taken together, these data suggest impairment of T cell receptor signaling in the colonic epithelium of the SHR.

Table 2. *List of pathways associated with indicated hub genes*

| Pathway ID | Pathway Description | Gene Count | FDR | Matching Proteins in the Network (Labels) |
|---|---|---|---|---|
| | | | *Lck* | |
| 4660 | T cell receptor signaling pathway | 9 | 6.71E-12 | CD3E,CD3G,CD8A,ITK,LAT,LCK,LCP2,PIK3CD,ZAP70 |
| 4650 | natural killer cell-mediated cytotoxicity | 8 | 1.81E-09 | CD48,KLRK1,LAT,LCK,LCP2,PIK3CD,TYROBP,ZAP70 |
| 5340 | primary immunodeficiency | 5 | 2.03E-07 | CD3E,CD8A,IL2RG,LCK,ZAP70 |
| | | | *Gng4* | |
| 4062 | chemokine signaling pathway | 8 | 5.61E-10 | ADCY7,CCL20,CCL5,CXCR4,GNG2,GNG4,PIK3CD,PREX1 |
| 4080 | neuroactive ligand-receptor interaction | 7 | 3.97E-07 | CALCRL,CHRM3,F2R,GABBR1,P2RY2,PTGER3,SSTR1 |
| 5032 | morphine addiction | 5 | 1.31E-06 | ADCY7,GABBR1,GNG2,GNG4,KCNJ5 |
| | | | *CD3g* | |
| 4660 | T cell receptor signaling pathway | 8 | 1.80E-11 | CD3E,CD3G,CD8A,ITK,LAT,LCK,LCP2,ZAP70 |
| 5340 | primary immunodeficiency | 5 | 4.03E-08 | CD3E,CD8A,IL2RG,LCK,ZAP70 |
| 4650 | natural killer cell-mediated cytotoxicity | 5 | 1.28E-05 | LAT,LCK,LCP2,PRF1,ZAP70 |
| | | | *Zap70* | |
| 4660 | T cell receptor signaling pathway | 9 | 1.28E-15 | CD3E,CD3G,CD8A,ITK,LAT,LCK,LCP2,PIK3CD,ZAP70 |
| 4650 | natural killer cell-mediated cytotoxicity | 6 | 2.87E-08 | LAT,LCK,LCP2,PIK3CD,TYROBP,ZAP70 |
| 5340 | primary immunodeficiency | 4 | 9.25E-07 | CD3E,CD8A,LCK,ZAP70 |
| | | | *Il2rb* | |
| 5166 | HTLV-I infection | 6 | 2.49E-06 | CD3G,IL2RA,IL2RB,IL2RG,LCK,PIK3CD |
| 5162 | measles | 5 | 2.53E-06 | CD3G,IL2RA,IL2RB,IL2RG,PIK3CD |
| 4660 | T cell receptor signaling pathway | 4 | 4.57E-05 | CD3G,CD8A,LCK,PIK3CD |
| 4650 | natural killer cell-mediated cytotoxicity | 4 | 8.53E-05 | GZMB,LCK,PIK3CD,PRF1 |

Hub genes with significant differences between WKY and SHR colonic epithelium are associated with the T cell receptor (TCR) signaling pathway. Pathway ID is an identified pathway number from an integrated pathway database of KEGG. Gene count is the number of genes involved in the indicated pathway. The proteins expressed by the pathway relevant genes are listed in the last column, matching proteins in the network. FDR, false discovery rate.

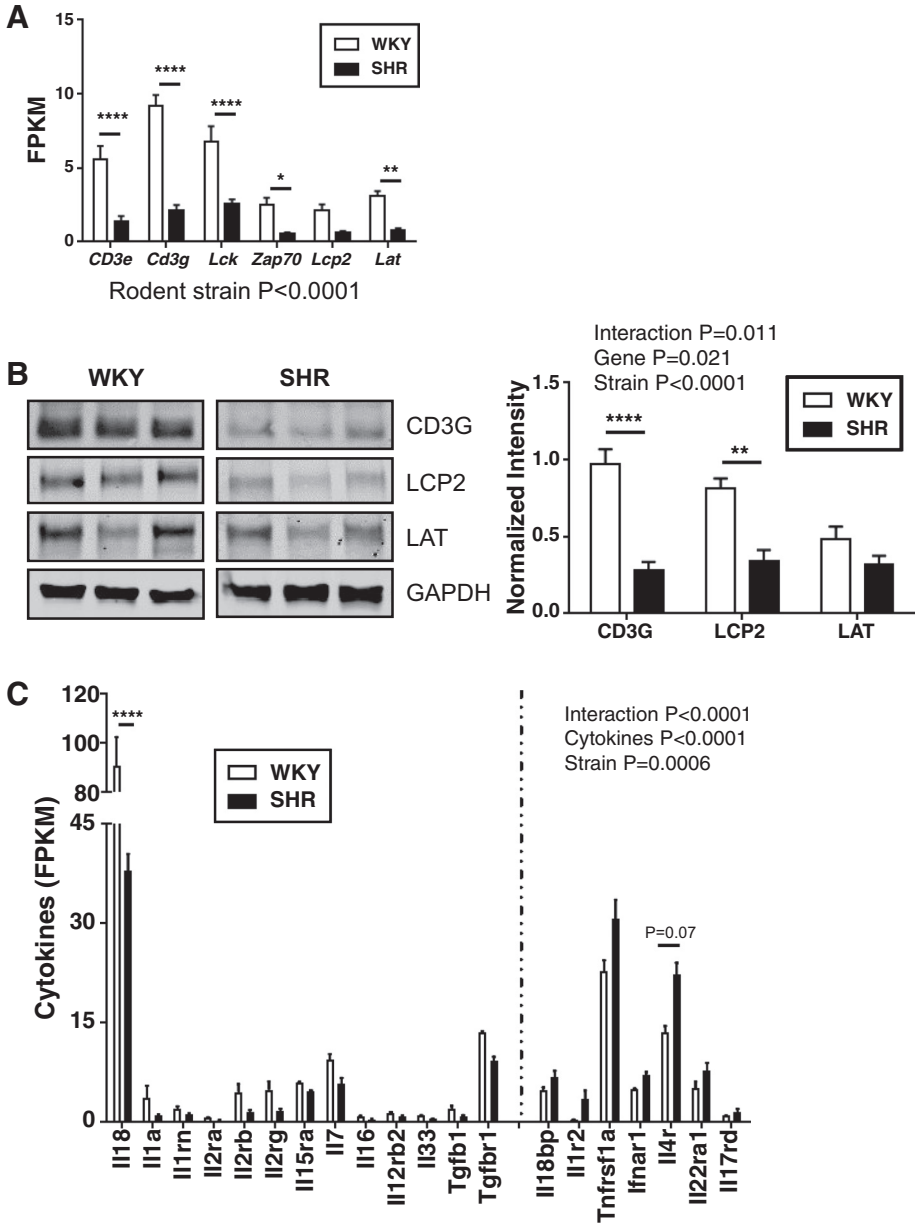


Fig. 3. Suppressed expression of genes in the T cell receptor (TCR) signaling pathway in the colonic epithelium of SHR. *A*: reduced expression of genes in the TCR signaling pathway. FPKM, fragments per kilobase million ($n = 4$/group). *B*: suppression of proteins in the TCR signaling pathway ($n = 3$/group). Quantification data were obtained by measuring the intensity of the Western blot band for indicated proteins. *C*: differential expression of cytokines between WKY and SHR ($n = 4$/group). Higher or lower expression of cytokines in the SHR was separated by a dashed line. In all three panels, statistical analysis was performed by two-way ANOVA analysis followed by Sidak's multiple comparison test $^{*}P < 0.05$, $^{**}P < 0.01$, $^{****}P < 0.0001$.

*Altered cytokine expression pattern in the colonic epithelium of SHR.* Next, we analyzed cytokine expression profiles to evaluate the potential impact of altered TCR signaling in the colonic epithelium of SHR. The interaction of two factors (cytokine, strain) differs significantly. In addition, the profile of a variety of cytokines significantly differed between the two strains, as indicated by strain factor $P < 0.05$ (Fig. 3*C*). Acute (innate) immune response cytokines of the IL1 family (e.g., *Il18*, *Il1a*) were dominant in the WKY. In contrast, SHR expressed more antagonist molecules (e.g., *Il18bp*, *Il1r2*) of the IL1 family cytokines. Interestingly, the expression of the Tnf superfamily receptor 1a was higher in the SHR (Fig. 3*C*). Higher expression of the cytokines and receptors responsible for lymphocyte proliferation, differentiation, and activation, (e.g., *Il12* receptor, *Il15ra*, *Il7*, *Il16*, *Tgfb1*) was found in the WKY, while cytokine receptors for production of antimicrobials, Th2 and Th17 cells (e.g., *Il22ra1, Il4r*, and *Il17rd*) were higher in the SHR (Fig. 3*C*).

*Higher TCR $\alpha\beta^+$ cell population in the colonic epithelium and MLN of SHR.* Since TCR signaling components were less expressed in the SHR, we determined if this could be due to a reduction in TCR $\alpha\beta^+$ cells. The gating strategies for colon, MLN and spleen are illustrated in Supplemental Fig. S3. Surprisingly, we observed significantly more TCR $\alpha\beta^+$ cells in the colonic epithelium layer of SHR compared with WKY (Fig. 4*A*). No differences in the proportions of epithelial cell populations were found between WKY and SHR in the colonic epithelium layer (Supplemental Fig. S4A). MLN, major lymph nodes collecting intestine-derived lymph, is the organ where immune responses are stimulated by gut antigens. Since the MLNs constantly supply activated T cells to the gut epithelium (31), we also investigated the TCR $\alpha\beta^+$ cell population in the MLNs. Consistent with colonic epithelium, we observed significantly more TCR $\alpha\beta^+$ cells in the SHR MLN (Fig. 4*B*). Last, we evaluated the TCR $\alpha\beta^+$ cell population in the spleen. The spleen is a secondary immune organ responsible for

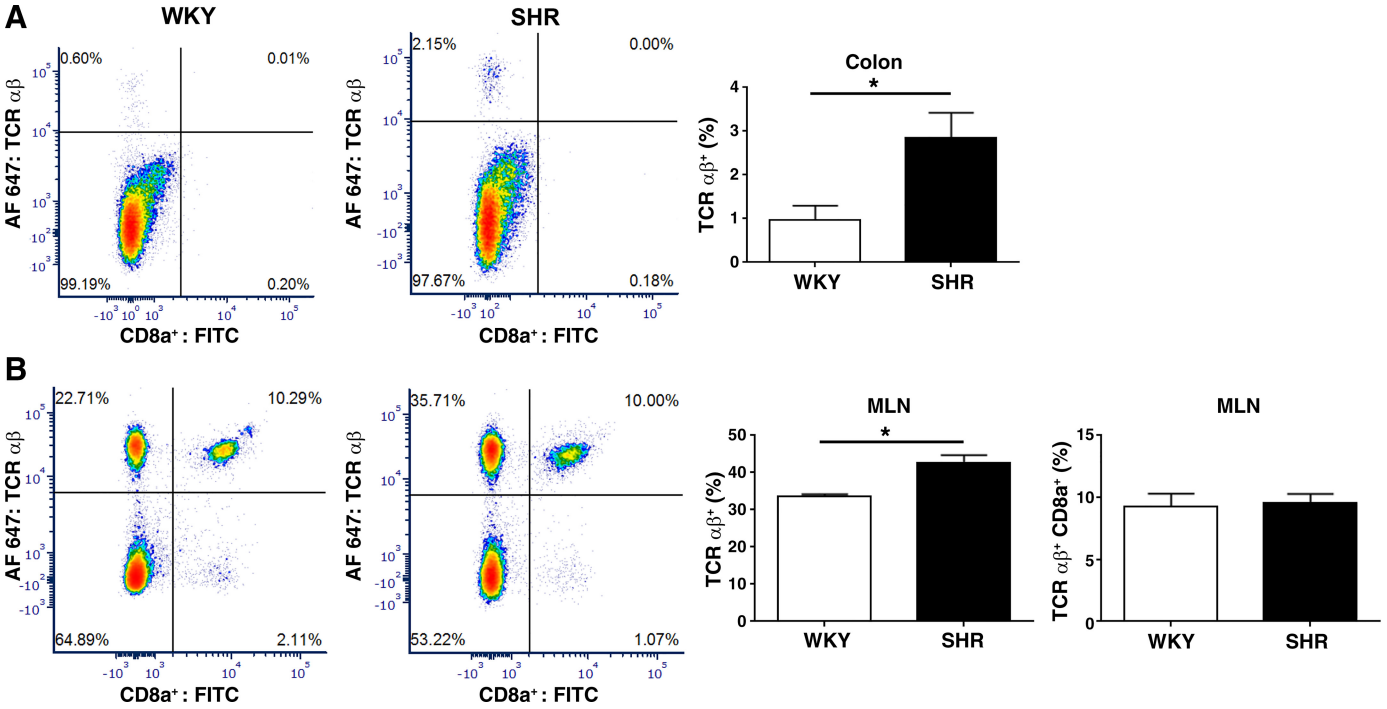


Fig. 4. Abundance of $\alpha\beta^+$ T cells in the colonic epithelium and mesenteric lymph nodes (MLN) of SHR. *A*: abundance of colonic $\alpha\beta^+$ T cells in the SHR epithelium. Isolated cells from epithelium were stained and analyzed by flow cytometry. *B*: more TCR$\alpha\beta^+$ cells in the SHR MLN. Single cell suspension from MLN was prepared and stained before flow cytometry analysis. TCR$\alpha\beta^+$ cells were gated using a total live cell population. Data are presented as percentages of indicated cell populations of total live cells. Statistical analysis was performed by unpaired *t* test * $P < 0.05$. $n = 4$/group.

production of hematopoietic cells and filtration of blood in systemic circulation. We did not observe a significant difference in the TCR $\alpha\beta^+$ cell population between WKY and SHR in the spleen (Supplemental Fig. S4B). Interestingly, there were significantly more TCR $\alpha\beta^+$ CD8a$^+$ cells in the spleen of the SHR (Supplemental Fig. S4B).

$\gamma\delta$ TCR functions with a variety of co-receptors and downstream molecules, few of which are shared by $\alpha\beta$ TCR signaling (41). The functions of these shared molecules are still obscure in $\gamma\delta$ TCR signaling and apparently different from those of $\alpha\beta$ TCR signaling (25, 45). Despite the discrepancy, we tested the abundance of TCR $\gamma\delta^+$ cells in the colonic epithelium, MLN, and spleen. Interestingly, we found significantly fewer TCR $\gamma\delta^+$ cells in the spleen and a trend toward fewer of the other two immune compartments in the SHR (Supplemental Fig. S5). However, the percentages of TCR $\gamma\delta^+$ cells were relatively low compared with TCR $\alpha\beta^+$ cells. Therefore, the contribution of TCR $\gamma\delta^+$ cells to suppressed canonical TCR signaling would appear to be insignificant. In summary, our data suggest that the suppressed TCR signaling pathway in the SHR colonic epithelium is not due to a reduction in TCR $\alpha\beta^+$ cells.

*Lower Alpi expression in colonic epithelium of SHR. Alpi* encodes IAP, which is predominantly located in gut epithelial cells (13). The expression profile showed ~2,000-fold lower expression of Alpi in the SHR (Fig. 5*A*). Immunohistochemical analysis showed significantly less IAP staining in the epithelial layer of the SHR gut compared with the WKY (Fig. 5*B*). Lower *Alpi* expression and IAP protein suggests that the ability of the SHR intestinal epithelium to counteract bacteria-derived LPS toxicity and protect against inflammation is significantly compromised.

## DISCUSSION

The most significant finding of the study is that the colonic epithelium from hypertensive rats displays significant changes that include intrinsic suppression of the $\alpha\beta$ TCR signaling pathway, lower expression of cytokines and receptors linked to lymphocyte proliferation, activation and differentiation, and less IAP. These changes, coupled with disrupted intestinal barrier function and microbial dysbiosis (43, 57), suggest that a unique gut microenvironment is key in altered gut-microbiota communication in hypertension.

We focused on the proximal colonic epithelium, a site adjacent to the metabolically active cecum in rodents. Our RNA-Seq data demonstrated *1*) transcriptional and posttranscriptional suppression of components of the $\alpha\beta$ TCR signaling pathway without decreased TCR $\alpha\beta^+$ cells in the colonic epithelium of the SHR, *2*) a tendency for lower $\gamma\delta^+$ TCR cells in the SHR from both colonic epithelium and MLN, and *3*) profoundly less ALPI in the SHR epithelium. These observations are the first demonstration of transcriptional alterations in gut epithelium linked to hypertension. Given the functional divergence, further study is needed to address whether these changes in the colonic epithelium are consistent throughout gastrointestinal segments or specific to this segment.

Most of the hub genes we identified in the network of genes with predominantly lower expression in the SHR are highly involved in the TCR signaling pathway. There are two types of TCR$^+$ IEL, $\alpha\beta$ and $\gamma\delta$ T cells (36). The genes with lower expression in the SHR are mainly downstream components of the canonical $\alpha\beta$ TCR signaling pathway. We demonstrated a consistently lower expression of these genes at transcriptional and posttranscriptional levels in the SHR. This was not due to

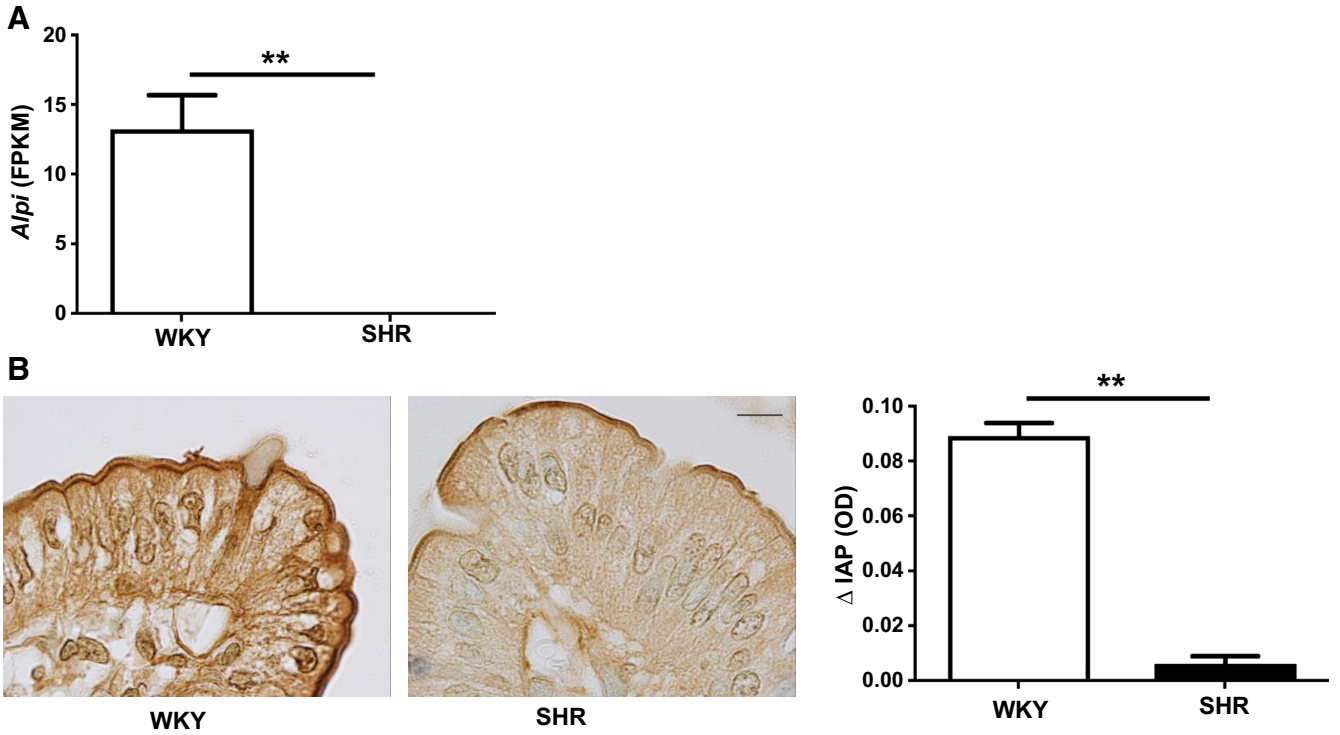


Fig. 5. Lower *Alpi* gene expression and intestinal alkaline phosphatase in the colonic epithelium of SHR. *A*: *Alpi* transcripts presented as FPKM from RNA-Seq data. *B*: immunohistochemical staining of in intestinal alkaline phosphatase (IAP) in WKY and SHR colonic epithelium. Statistical analysis was performed by unpaired *t* test $^{**}P < 0.01$. $n = 4$/group.

fewer αβ TCR$^+$ cells, suggesting lower expression of TCR signaling molecules was not due to reduced TCR$^+$ IEL cell number, but a result of intrinsic suppression of TCR signaling components in the SHR epithelium. Consistent with this, we found a lower expression of *Il2* receptor, suggesting less activation and differentiation of effector lymphocytes in the SHR epithelium (33).

In contrast to αβ T cells, limited numbers of genes of the canonical αβ TCR signaling pathway have been reported to be involved in γδ TCR signaling (41). We observed a trend toward fewer γδ T cells in the epithelium and MLN of SHR. It has been reported that mice deficient in γδ T cells have structural differences within their intestine, such as reduced proliferation of epithelial cells and tight junction proteins (34). Hoytema van Konijnenburg et al. (17) found that γδ TCR IELs exhibit unique microbiota-dependent location and movement patterns in the epithelial compartment, along with metabolic changes in γδ TCR IELs exposed to different pathogens. These data suggest a role for γδ T cells in limiting transepithelial pathogen invasion (10, 12). Thus, it is tempting to suggest that fewer γδ T cells in SHR epithelium and MLN may lead to deficient responses of intestinal immune cells to microbes. However, this view is in contrast to a recent report showing increased γδ T cells in angiotensin II-induced vascular injury (3). The difference in these two observations may be due to the fact that γδ T cell subsets function in tissue-specific and microenvironment-dependent fashions (28). Further studies would be required to dissect the γδ T cell repertoire in the context of hypertension.

The reduced TCR signaling in IELs seems to contradict the increased intestinal inflammation observed in the SHR (43). However, our subsequent analysis of the cytokine profile in colonic epithelium suggested a shift between IL1 family- and TNF family-mediated acute immune responses between WKY and SHR. IL1 family signaling was abundant in the WKY and TNF family signaling was enriched in the SHR. Cytokines responsible for proliferation (19, 47), differentiation (27, 42), migration (18, 21), and activation (42) of lymphocytes were increased in WKY. For example, *Tgfb1*, encoding TGFβ, is an essential cytokine for generation and modulation of functional regulatory T cells. TGFβ binding to TGFβ receptor 1 is necessary to suppress proinflammatory Th17 cells (24). Combined with the fact that the expression of *Il6* is comparable between WKY and SHR (data not shown), it is speculated that the Th17 cell population is reduced in the WKY colon compared with the SHR. This is consistent with previous publications that there were significantly more Th17$^+$ cells in serum of hypertensive patients (23, 52). This suggested a more delicate regulatory mechanism in the colonic epithelium in the WKY. In contrast, the expression of genes responsible for antiproliferation (22) and propermeability (4) for epithelial cells and proinflammation for neutrophils (32) was abundant in the SHR epithelium. Interestingly, we also observed more *Il22r* transcription in the SHR. Since IL22 receptor is exclusively expressed on epithelial cells, this indicates a protective and regenerative demand of SHR epithelial cells (37). Therefore, the suppressed TCR pathway in SHR was accompanied by a serial of innate immune responses, including enriched TNFα signaling, a disrupted intestinal epithelial barrier, and an innate immunity-derived proinflammatory epithelial microenvironment.

The enrichment of biological processes relevant to response to intestinal bacteria or molecules in the SHR correlates with our previous finding that SHR harbors dysbiotic microbiota (57). This suggests a dysregulated interaction between gut microbiota and gut epithelium in the SHR. In addition, enriched responses to bacteria are attributable to genes involved in mainly innate immunity, such as *Cfh*, *Ace*, *Reg3b*, *Anxa3*, *Tlr5*, *Areg*, *Hmgb2*, *Ccl20*, etc. (supplement 1). Less Alpi is especially relevant in this respect. IAP, the protein product of *Alpi*, is specific to gut epithelial cells and plays an important role in the maintenance of gut barrier function (38), mucosal immunity (38), microbiota eubiosis (29), and physiological homeostasis (9, 20) and serves as a primary line of defense against bacterial stimuli like LPS (58). Indeed, response to LPS was one of only three enriched processes modeled from the SHR transcriptomic results and suggests that the immune function of the epithelium is stimulated by the lack of LPS detoxification by the ALPI-deficient SHR epithelial cells. Also, ALPI knockout mice have enhanced LPS signaling pathway (13), decreased microbiota diversity (29), and dysfunctional mucosal barrier (13); all of these changes are also seen in hypertension (23, 43). This suggests a trend toward immune overreaction of gut epithelium to its dysbiotic gut microbiota in hypertension. In contrast, WKY harbors a balanced gut microbiota (57) and appropriate regulatory immune responses in the epithelium (Table 1). Therefore, our current study demonstrated significantly suppressed TCR signaling in the SHR intestinal epithelium.

Finally, an important question is whether these changes in the gut are the cause or result of hypertension. No conclusive evidence is available in support of either view. However, our data with prehypertensive SHR indicate that certain changes in the gut occur before any increase in blood pressure. Prehypertensive SHR show enhanced sympathetic nerve activity to the gut (43), fewer tight junction proteins, and more of certain inflammatory cytokines. This would suggest that sympathetic regulation of gut barrier function could be the initial step in a complex sequence of events in gut-microbiota communication in hypertension.

In conclusion, our study shows fewer TCR signaling components and IAP, and a trend toward fewer γδ T cells in the colonic epithelium of SHR. This is consistent with reported dysfunctions in the gut including dysbiosis (57), increased permeability (23, 43) immune responses (48, 61), and imbalanced microbial metabolites (5, 50, 54) in hypertension. In addition, we found perturbed TCR signaling in the colonic epithelium of SHR. Taken together, these observations suggest that prohypertensive signals may exert influences on intestinal epithelium to alter host gut-microbiota interactions in hypertension.

## ACKNOWLEDGMENTS

We acknowledge technical support for RNA-Seq library construction, next-generation Illumina HiSeq 3000 sequencing, and RNA-Seq bioinformatic analysis at the Interdisciplinary Center for Biotechnology Research (ICBR) Gene Expression & Genotyping core, NextGen DNA Sequencing core, and Bioinformatics core, University of Florida.

## GRANTS

This study was supported by National Heart, Lung, and Blood Institute Grants R01 HL-132448 and HL-033610 to M. K. Raizada, a Biocodex Microbiota Foundation USA grant to T. Yang, and National Natural Science Foundation of China Grant 81700373 to H. Li.

## DISCLOSURES

No conflicts of interest, financial or otherwise, are declared by the authors.

## AUTHOR CONTRIBUTIONS

T.Y. and M.K.R. conceived and designed research; T.Y., H.-B.L., A.C.O., and R.G. performed experiments; T.Y., H.-B.L., and A.C.O. analyzed data; T.Y., A.C.O., E.M.R., and M.K.R. interpreted results of experiments; T.Y. and A.C.O. prepared figures; T.Y. and E.M.R. drafted manuscript; T.Y., A.C.O., E.M.R., C.J.P., and M.K.R. edited and revised manuscript; T.Y., A.C.O., R.G., H.-B.L., E.M.R., C.J.P., and M.K.R. approved final version of manuscript.

## REFERENCES

1. **Allen J, Sears CL.** Impact of the gut microbiome on the genome and epigenome of colon epithelial cells: contributions to colorectal cancer development. *Genome Med* 11: 11, 2019. doi:10.1186/s13073-019-0621-2.
2. **Bolger AM, Lohse M, Usadel B.** Trimmomatic: a flexible trimmer for Illumina sequence data. *Bioinformatics* 30: 2114–2120, 2014. doi:10.1093/bioinformatics/btu170.
3. **Caillon A, Mian MOR, Fraulob-Aquino JC, Huo KG, Barhoumi T, Ouerd S, Sinnaeve PR, Paradis P, Schiffrin EL.** γδ T Cells Mediate Angiotensin II-Induced Hypertension and Vascular Injury. *Circulation* 135: 2155–2162, 2017. doi:10.1161/CIRCULATIONAHA.116.027058.
4. **Ceponis PJ, Botelho F, Richards CD, McKay DM.** Interleukins 4 and 13 increase intestinal epithelial permeability by a phosphatidylinositol 3-kinase pathway. Lack of evidence for STAT 6 involvement. *J Biol Chem* 275: 29132–29137, 2000. doi:10.1074/jbc.M003516200.
5. **Chakraborty S, Galla S, Cheng X, Yeo JY, Mell B, Singh V, Yeoh B, Saha P, Mathew AV, Vijay-Kumar M, Joe B.** Salt-Responsive Metabolite, β-Hydroxybutyrate, Attenuates Hypertension. *Cell Reports* 25: 677–689.e4, 2018. doi:10.1016/j.celrep.2018.09.058.
6. **Cheroutre H, Lambolez F, Mucida D.** The light and dark sides of intestinal intraepithelial lymphocytes. *Nat Rev Immunol* 11: 445–456, 2011. doi:10.1038/nri3007.
7. **Dobin A, Davis CA, Schlesinger F, Drenkow J, Zaleski C, Jha S, Batut P, Chaisson M, Gingeras TR.** STAR: ultrafast universal RNA-seq aligner. *Bioinformatics* 29: 15–21, 2013. doi:10.1093/bioinformatics/bts635.
8. **Durgan DJ, Ganesh BP, Cope JL, Ajami NJ, Phillips SC, Petrosino JF, Hollister EB, Bryan RM Jr.** Role of the Gut Microbiome in Obstructive Sleep Apnea-Induced Hypertension. *Hypertension* 67: 469–474, 2016. doi:10.1161/HYPERTENSIONAHA.115.06672.
9. **Economopoulos KP, Ward NL, Phillips CD, Teshager A, Patel P, Mohamed MM, Hakimian S, Cox SB, Ahmed R, Moaven O, Kaliannan K, Alam SN, Haller JF, Goldstein AM, Bhan AK, Malo MS, Hodin RA.** Prevention of antibiotic-associated metabolic syndrome in mice by intestinal alkaline phosphatase. *Diabetes Obes Metab* 18: 519–527, 2016. doi:10.1111/dom.12645.
10. **Edelblum KL, Singh G, Odenwald MA, Lingaraju A, El Bissati K, McLeod R, Sperling AI, Turner JR.** γδ Intraepithelial Lymphocyte Migration Limits Transepithelial Pathogen Invasion and Systemic Disease in Mice. *Gastroenterology* 148: 1417–1426, 2015. doi:10.1053/j.gastro.2015.02.053.
11. **FastQC.** http://www.bioinformatics.babraham.ac.uk/projects/fastqc/.
12. **Fuell C, Kober OI, Hautefort I, Juge N.** Mice deficient in intestinal γδ intraepithelial lymphocytes display an altered intestinal O-glycan profile compared with wild-type littermates. *Glycobiology* 25: 42–54, 2015. doi:10.1093/glycob/cwu088.
13. **Goldberg RF, Austen WG Jr, Zhang X, Munene G, Mostafa G, Biswas S, McCormack M, Eberlin KR, Nguyen JT, Tatlidede HS, Warren HS, Narisawa S, Millán JL, Hodin RA.** Intestinal alkaline phosphatase is a gut mucosal defense factor maintained by enteral nutrition. *Proc Natl Acad Sci USA* 105: 3551–3556, 2008. doi:10.1073/pnas.0712140105.
14. **Gorfu G, Rivera-Nieves J, Ley K.** Role of beta7 integrins in intestinal lymphocyte homing and retention. *Curr Mol Med* 9: 836–850, 2009. doi:10.2174/156652409789105525.
15. **Gracz AD, Puthoff BJ, Magness ST.** Identification, isolation, and culture of intestinal epithelial stem cells from murine intestine. *Methods Mol Biol* 879: 89–107, 2012. doi:10.1007/978-1-61779-815-3_6.

16. **Guy-Grand D, Griscelli C, Vassalli P.** The gut-associated lymphoid system: nature and properties of the large dividing cells. *Eur J Immunol* 4: 435–443, 1974. doi:10.1002/eji.1830040610.
17. **Hoytema van Konijnenburg DP, Reis BS, Pedicord VA, Farache J, Victora GD, Mucida D.** Intestinal Epithelial and Intraepithelial T Cell Crosstalk Mediates a Dynamic Response to Infection. *Cell* 171: 783–794.e13, 2017. doi:10.1016/j.cell.2017.08.046.
18. **Hu MD, Ethridge AD, Lipstein R, Kumar S, Wang Y, Jabri B, Turner JR, Edelblum KL.** Epithelial IL-15 Is a Critical Regulator of γδ Intraepithelial Lymphocyte Motility within the Intestinal Mucosa. *J Immunol* 201: 747–756, 2018. doi:10.4049/jimmunol.1701603.
19. **Inoue S, Unsinger J, Davis CG, Muenzer JT, Ferguson TA, Chang K, Osborne DF, Clark AT, Coopersmith CM, McDunn JE, Hotchkiss RS.** IL-15 prevents apoptosis, reverses innate and adaptive immune dysfunction, and improves survival in sepsis. *J Immunol* 184: 1401–1409, 2010. doi:10.4049/jimmunol.0902307.
20. **Kaliannan K, Hamarneh SR, Economopoulos KP, Nasrin Alam S, Moaven O, Patel P, Malo NS, Ray M, Abtahi SM, Muhammad N, Raychowdhury A, Teshager A, Mohamed MM, Moss AK, Ahmed R, Hakimian S, Narisawa S, Millán JL, Hohmann E, Warren HS, Bhan AK, Malo MS, Hodin RA.** Intestinal alkaline phosphatase prevents metabolic syndrome in mice. *Proc Natl Acad Sci USA* 110: 7003–7008, 2013. doi:10.1073/pnas.1220180110.
21. **Kaser A, Dunzendorfer S, Offner FA, Ludwiczek O, Enrich B, Koch RO, Cruikshank WW, Wiedermann CJ, Tilg H.** B lymphocyte-derived IL-16 attracts dendritic cells and Th cells. *J Immunol* 165: 2474–2480, 2000. doi:10.4049/jimmunol.165.5.2474.
22. **Katlinskaya YV, Katlinski KV, Lasri A, Li N, Beiting DP, Durham AC, Yang T, Pikarsky E, Lengner CJ, Johnson FB, Ben-Neriah Y, Fuchs SY.** Type I Interferons Control Proliferation and Function of the Intestinal Epithelium. *Mol Cell Biol* 36: 1124–1135, 2016. doi:10.1128/MCB.00988-15.
23. **Kim S, Goel R, Kumar A, Qi Y, Lobaton G, Hosaka K, Mohammed M, Handberg EM, Richards EM, Pepine CJ, Raizada MK.** Imbalance of gut microbiome and intestinal epithelial barrier dysfunction in patients with high blood pressure. *Clin Sci (Lond)* 132: 701–718, 2018. doi:10.1042/CS20180087.
24. **Konkel JE, Zhang D, Zanvit P, Chia C, Zangarle-Murray T, Jin W, Wang S, Chen W.** Transforming Growth Factor-β Signaling in Regulatory T Cells Controls T Helper-17 Cells and Tissue-Specific Immune Responses. *Immunity* 46: 660–674, 2017. doi:10.1016/j.immuni.2017.03.015.
25. **Kuhns MS, Badgandi HB.** Piecing together the family portrait of TCR-CD3 complexes. *Immunol Rev* 250: 120–143, 2012. doi:10.1111/imr.12000.
26. **Li J, Zhao F, Wang Y, Chen J, Tao J, Tian G, Wu S, Liu W, Cui Q, Geng B, Zhang W, Weldon R, Auguste K, Yang L, Liu X, Chen L, Yang X, Zhu B, Cai J.** Gut microbiota dysbiosis contributes to the development of hypertension. *Microbiome* 5: 14, 2017. doi:10.1186/s40168-016-0222-x.
27. **Mahapatro M, Foersch S, Hefele M, He GW, Giner-Ventura E, Mchedlidze T, Kindermann M, Vetrano S, Danese S, Günther C, Neurath MF, Wirtz S, Becker C.** Programming of Intestinal Epithelial Differentiation by IL-33 Derived from Pericryptal Fibroblasts in Response to Systemic Infection. *Cell Reports* 15: 1743–1756, 2016. doi:10.1016/j.celrep.2016.04.049.
28. **Malik S, Want MY, Awasthi A.** The Emerging Roles of Gamma-Delta T Cells in Tissue Inflammation in Experimental Autoimmune Encephalomyelitis. *Front Immunol* 7: 14, 2016. doi:10.3389/fimmu.2016.00014.
29. **Malo MS, Alam SN, Mostafa G, Zeller SJ, Johnson PV, Mohammad N, Chen KT, Moss AK, Ramasamy S, Faruqui A, Hodin S, Malo PS, Ebrahimi F, Biswas B, Narisawa S, Millán JL, Warren HS, Kaplan JB, Kitts CL, Hohmann EL, Hodin RA.** Intestinal alkaline phosphatase preserves the normal homeostasis of gut microbiota. *Gut* 59: 1476–1484, 2010. doi:10.1136/gut.2010.211706.
30. **Mayassi T, Jabri B.** Human intraepithelial lymphocytes. *Mucosal Immunol* 11: 1281–1289, 2018. doi:10.1038/s41385-018-0016-5.
31. **McDermott MR, Horsewood P, Clark DA, Bienenstock J.** T lymphocytes in the intestinal epithelium and lamina propria of mice. *Immunology* 57: 213–218, 1986.
32. **Mellett M, Atzei P, Horgan A, Hams E, Floss T, Wurst W, Fallon PG, Moynagh PN.** Orphan receptor IL-17RD tunes IL-17A signalling and is required for neutrophilia. *Nat Commun* 3: 1119, 2012. doi:10.1038/ncomms2127.
33. **Mitra S, Ring AM, Amarnath S, Spangler JB, Li P, Ju W, Fischer S, Oh J, Spolski R, Weiskopf K, Kohrt H, Foley JE, Rajagopalan S, Long EO, Fowler DH, Waldmann TA, Garcia KC, Leonard WJ.** Interleukin-2 activity can be fine tuned with engineered receptor signaling clamps. *Immunity* 42: 826–838, 2015. doi:10.1016/j.immuni.2015.04.018.
34. **Nielsen MM, Witherden DA, Havran WL.** γδ T cells in homeostasis and host defence of epithelial barrier tissues. *Nat Rev Immunol* 17: 733–745, 2017. doi:10.1038/nri.2017.101.
35. **Norlander AE, Madhur MS, Harrison DG.** The immunology of hypertension. *J Exp Med* 215: 21–33, 2018. doi:10.1084/jem.20171773.
36. **Olivares-Villagómez D, Van Kaer L.** Intestinal Intraepithelial Lymphocytes: Sentinels of the Mucosal Barrier. *Trends Immunol* 39: 264–275, 2018. doi:10.1016/j.it.2017.11.003.
37. **Parks OB, Pociask DA, Hodzic Z, Kolls JK, Good M.** Interleukin-22 Signaling in the Regulation of Intestinal Health and Disease. *Front Cell Dev Biol* 3: 85, 2016. doi:10.3389/fcell.2015.00085.
38. **Parlato M, Charbit-Henrion F, Pan J, Romano C, Duclaux-Loras R, Le Du MH, Warner N, Francalanci P, Bruneau J, Bras M, Zarhrate M, Bègue B, Guegan N, Rakotobe S, Kapel N, De Angelis P, Griffiths AM, Fiedler K, Crowley E, Ruemmele F, Muise AM, Cerf-Bensussan N.** Human ALPI deficiency causes inflammatory bowel disease and highlights a key mechanism of gut homeostasis. *EMBO Mol Med* 10: e8483, 2018. doi:10.15252/emmm.201708483.
39. **Qin Y, Wade PA.** Crosstalk between the microbiome and epigenome: messages from bugs. *J Biochem* 163: 105–112, 2018. doi:10.1093/jb/mvx080.
40. **Regner EH, Ohri N, Stahly A, Gerich ME, Fennimore BP, Ir D, Jubair WK, Görg C, Siebert J, Robertson CE, Caplan L, Frank DN, Kuhn KA.** Functional intraepithelial lymphocyte changes in inflammatory bowel disease and spondyloarthritis have disease specific correlations with intestinal microbiota. *Arthritis Res Ther* 20: 149, 2018. doi:10.1186/s13075-018-1639-3.
41. **Ribeiro ST, Ribot JC, Silva-Santos B.** Five Layers of Receptor Signaling in γδ T-Cell Differentiation and Activation. *Front Immunol* 6: 15, 2015. doi:10.3389/fimmu.2015.00015.
42. **Ross SH, Cantrell DA.** Signaling and Function of Interleukin-2 in T Lymphocytes. *Annu Rev Immunol* 36: 411–433, 2018. doi:10.1146/annurev-immunol-042617-053352.
43. **Santisteban MM, Qi Y, Zubcevic J, Kim S, Yang T, Shenoy V, Cole-Jeffrey CT, Lobaton GO, Stewart DC, Rubiano A, Simmons CS, Garcia-Pereira F, Johnson RD, Pepine CJ, Raizada MK.** Hypertension-Linked Pathophysiological Alterations in the Gut. *Circ Res* 120: 312–323, 2017. doi:10.1161/CIRCRESAHA.116.309006.
44. **Setty M, Discepolo V, Abadie V, Kamhawi S, Mayassi T, Kent A, Ciszewski C, Maglio M, Kistner E, Bhagat G, Semrad C, Kupfer SS, Green PH, Guandalini S, Troncone R, Murray JA, Turner JR, Jabri B.** Distinct and Synergistic Contributions of Epithelial Stress and Adaptive Immunity to Functions of Intraepithelial Killer Cells and Active Celiac Disease. *Gastroenterology* 149: 681–691.e10, 2015. doi:10.1053/j.gastro.2015.05.013.
45. **Sullivan SA, Zhu M, Bao S, Lewis CA, Ou-Yang CW, Zhang W.** The role of LAT-PLCγ1 interaction in γδ T cell development and homeostasis. *J Immunol* 192: 2865–2874, 2014. doi:10.4049/jimmunol.1302493.
46. **Szklarczyk D, Franceschini A, Wyder S, Forslund K, Heller D, Huerta-Cepas J, Simonovic M, Roth A, Santos A, Tsafou KP, Kuhn M, Bork P, Jensen LJ, von Mering C.** STRING v10: protein-protein interaction networks, integrated over the tree of life. *Nucleic Acids Res* 43, *D1*: D447–D452, 2015. doi:10.1093/nar/gku1003.
47. **Tan JT, Dudl E, LeRoy E, Murray R, Sprent J, Weinberg KI, Surh CD.** IL-7 is critical for homeostatic proliferation and survival of naive T cells. *Proc Natl Acad Sci USA* 98: 8732–8737, 2001. doi:10.1073/pnas.161126098.
48. **Toral M, Robles-Vera I, de la Visitación N, Romero M, Sánchez M, Gómez-Guzmán M, Rodriguez-Nogales A, Yang T, Jiménez R, Algieri F, Gálvez J, Raizada MK, Duarte J.** Role of the immune system in vascular function and blood pressure control induced by faecal microbiota transplantation in rats. *Acta Physiol (Oxf)* 227: e13285, 2019. doi:10.1111/apha.13285.
49. **Toral M, Robles-Vera I, de la Visitación N, Romero M, Yang T, Sánchez M, Gómez-Guzmán M, Jiménez R, Raizada MK, Duarte J.** Critical Role of the Interaction Gut Microbiota - Sympathetic Nervous System in the Regulation of Blood Pressure. *Front Physiol* 10: 231, 2019. doi:10.3389/fphys.2019.00231.
50. **Walejko JM, Kim S, Goel R, Handberg EM, Richards EM, Pepine CJ, Raizada MK.** Gut microbiota and serum metabolite differences in African Americans and White Americans with high blood pressure. *Int J Cardiol* 271: 336–339, 2018. doi:10.1016/j.ijcard.2018.04.074.

51. **Wang J, Duncan D, Shi Z, Zhang B.** WEB-based GEne SeT AnaLysis Toolkit (WebGestalt): update 2013. *Nucleic Acids Res* 41, *W1*: W77–W83, 2013. doi:10.1093/nar/gkt439.
52. **Wilck N, Matus MG, Kearney SM, Olesen SW, Forslund K, Bartolomaeus H, Haase S, Mähler A, Balogh A, Markó L, Vvedenskaya O, Kleiner FH, Tsvetkov D, Klug L, Costea PI, Sunagawa S, Maier L, Rakova N, Schatz V, Neubert P, Frätzer C, Krannich A, Gollasch M, Grohme DA, Côrte-Real BF, Gerlach RG, Basic M, Typas A, Wu C, Titze JM, Jantsch J, Boschmann M, Dechend R, Kleinewietfeld M, Kempa S, Bork P, Linker RA, Alm EJ, Müller DN.** Salt-responsive gut commensal modulates $T_H17$ axis and disease. *Nature* 551: 585–589, 2017. doi:10.1038/nature24628.
53. **Yang L, Liu C, Zhao W, He C, Ding J, Dai R, Xu K, Xiao L, Luo L, Liu S, Li W, Meng H.** Impaired Autophagy in Intestinal Epithelial Cells Alters Gut Microbiota and Host Immune Responses. *Appl Environ Microbiol* 84: e00880-18, 2018. doi:10.1128/AEM.00880-18.
54. **Yang T, Magee KL, Colon-Perez LM, Larkin R, Liao YS, Balazic E, Cowart JR, Arocha R, Redler T, Febo M, Vickroy T, Martyniuk CJ, Reznikov LR, Zubcevic J.** Impaired butyrate absorption in the proximal colon, low serum butyrate and diminished central effects of butyrate on blood pressure in spontaneously hypertensive rats. *Acta Physiol (Oxf)* 226: e13256, 2019. doi:10.1111/apha.13256.
55. **Yang T, Owen JL, Lightfoot YL, Kladde MP, Mohamadzadeh M.** Microbiota impact on the epigenetic regulation of colorectal cancer. *Trends Mol Med* 19: 714–725, 2013. doi:10.1016/j.molmed.2013.08.005.
56. **Yang T, Richards EM, Pepine CJ, Raizada MK.** The gut microbiota and the brain-gut-kidney axis in hypertension and chronic kidney disease. *Nat Rev Nephrol* 14: 442–456, 2018. doi:10.1038/s41581-018-0018-2.
57. **Yang T, Santisteban MM, Rodriguez V, Li E, Ahmari N, Carvajal JM, Zadeh M, Gong M, Qi Y, Zubcevic J, Sahay B, Pepine CJ, Raizada MK, Mohamadzadeh M.** Gut dysbiosis is linked to hypertension. *Hypertension* 65: 1331–1340, 2015. doi:10.1161/HYPERTENSIONAHA.115.05315.
58. **Yang Y, Wandler AM, Postlethwait JH, Guillemin K.** Dynamic Evolution of the LPS-Detoxifying Enzyme Intestinal Alkaline Phosphatase in Zebrafish and Other Vertebrates. *Front Immunol* 3: 314, 2012. doi:10.3389/fimmu.2012.00314.
59. **Yoo BB, Mazmanian SK.** The Enteric Network: Interactions between the Immune and Nervous Systems of the Gut. *Immunity* 46: 910–926, 2017. doi:10.1016/j.immuni.2017.05.011.
60. **Zhang B, Kirov S, Snoddy J.** WebGestalt: an integrated system for exploring gene sets in various biological contexts. *Nucleic Acids Res* 33, *Web Server*: W741-8, 2005. doi:10.1093/nar/gki475.
61. **Zubcevic J, Jun JY, Kim S, Perez PD, Afzal A, Shan Z, Li W, Santisteban MM, Yuan W, Febo M, Mocco J, Feng Y, Scott E, Baekey DM, Raizada MK.** Altered inflammatory response is associated with an impaired autonomic input to the bone marrow in the spontaneously hypertensive rat. *Hypertension* 63: 542–550, 2014. doi:10.1161/HYPERTENSIONAHA.113.02722.
62. **Zubcevic J, Richards EM, Yang T, Kim S, Sumners C, Pepine CJ, Raizada MK.** Impaired Autonomic Nervous System-Microbiome Circuit in Hypertension. *Circ Res* 125: 104–116, 2019. doi:10.1161/CIRCRESAHA.119.313965.